Mechanism of nonresonant energy transfer between ions in $SrF_2:Er^{3+}$

J. R. Wietfeldt, D. S. Moore,* B. M. Tissue, and J. C. Wright
Department of Chemistry, University of Wisconsin, Madison, Wisconsin 53706
(Received 10 October 1985)

The temperature and magnetic field dependence of the nonresonant energy transfer rate is measured for two ions that exist as a well-defined dimer in $SrF_2:Er^{3+}$. The two ions are crystallographically inequivalent, so the energy transfer can be observed directly and unique transfer rates are obtained without modeling the radial dependence of energy transfer. The transfer is shown to result from a single-phonon-assisted process at low temperatures and a two-phonon-assisted resonant or Orbach process at higher temperatures. No evidence is found for nonresonant two-phonon processes.

INTRODUCTION

The mechanism for nonresonant energy transfer between a donor and acceptor with small energy mismatches has been a subject of recent theoretical[1-3] and experimental interest.[4-15] Theoretical considerations have shown that energy transfer accompanied by a direct one-phonon process is not as efficient as two-phonon processes because of the low density of phonon states at low phonon energies.[1] Nonresonant two-site, nonresonant Raman one-site and resonant Orbach processes have all been identified as possible mechanisms for nonresonant energy transfer assisted by two phonons.[1-3] Theoretical estimates predicted that a resonant two-phonon-assisted Orbach process should be more important than nonresonant two-phonon or direct single-phonon processes in ruby.[1] Experimentally, laser-induced fluorescence line-narrowing experiments have provided the best guidance on the relative importance of the different mechanisms.[4-7] Such studies have shown that a nonresonant two-phonon process dominates the nonresonant energy transfer at small energy mismatches in PrF_3 and $LaF_3:Pr$, where resonant two-phonon processes are not possible,[4,6] while a direct single-phonon process controls the energy transfer in ruby.[5,7] Resonant two-phonon Orbach processes have been reported by a number of workers in those systems where suitable resonances are available.[9-13] They have been observed to limit the phonon lifetime in ruby at large excited-state populations,[14] and have been used to explain observed correlations between nonequilibrium resonance phonons and the intensity and kinetics of luminescence on the short-wavelength wing of the inhomogeneously broadened R_1 line of ruby.[15] All of the experiments measure energy-transfer rates between ions with differing radial separations, and a model for the radial dependence of the rate must be used to extract the parameters describing the transfer. Other simplifying assumptions and approximations must be made including approximations about back transfer and neglect of direct one-phonon processes or contributions from several mechanisms of transfer. The temperature dependence of resonant and nonresonant two-phonon-assisted energy-transfer processes often differ subtly and cannot be used to definitively distinguish the mechanism. The resonant and nonresonant two-phonon processes can be definitively distinguished by their dependence on the energy separation between resonant levels. There have been fluorescence line-narrowing experiments that show the growth of the inhomogeneous line is nonuniform after narrow-line excitation and depends on the energy difference from line center.[10] The dependence indicated a $1/(\Delta E)^2$ dependence and suggested the transfer mechanism was an Orbach process.

Fluorite-structure crystals doped with trivalent lanthanides offer some important advantages for energy-transfer studies. The lanthanide ions in these crystals are charge compensated by fluoride interstitial ions (F_i'). The different arrangements of the F_i' relative to a rare-earth dopant give rise to many different site symmetries for the rare earth. In $SrF_2:Er^{3+}$, it was found there were four possible sites for a single Er^{3+} ion compensated by one F_i'. At dopant concentrations above 0.05 mol %, at least five additional sites become important as the dipolar and strain interactions cause clustering of the rare-earth dopants and the F_i' charge compensations.[16] The clusters offer a favorable situation for studying energy transfer because the transitions of the individual ions that make up dimers or higher-order clusters are resolved and the energy transfer can be observed between ions with well-defined radial separations. One does not need to model the energy-transfer dependence on radial separation and perform an ensemble average over all separations in order to fit the experimental data. In this paper we study the energy transfer between two crystallographically inequivalent ions that are in a cluster labeled K.[16] Unique rate constants are obtained for the energy transfer between two levels that are separated by 31.3 cm^{-1}. The temperature variation of the rate constants shows that the mechanism for the nonresonant energy transfer is a one-phonon-assisted direct process at low temperatures and a two-phonon-assisted process at higher temperatures. Excellent fits to the data are obtained for both a resonant two-phonon Orbach process and a nonresonant two-phonon, two-site process and cannot distinguish between the mechanisms. An external magnetic field was used to change the level separations and the transfer rate changed dramatically. These experiments show definitively that an

Orbach process is responsible for the nonresonant energy transfer.

THEORY

The energy-level structure for the Er^{3+} ions studied in this paper is different from that treated theoretically for a resonant Orbach process in the Cr^{3+} system. In $Al_2O_3:Cr^{3+}$, the Cr^{3+} ions are equivalent and the resonant level for the two-phonon process was an excited state. The theoretical treatment for the nonresonant two-phonon and direct one-phonon-assisted processes is not affected by such differences, but the description of the resonant two-phonon Orbach process is changed because there are additional levels that can become resonant with a phonon. The relevant energy-level structure is sketched in Fig. 1. An expression for the Orbach process can be obtained by the extension of the treatment used by Holstein, Lyo, and Orbach.[3] The energy-transfer rate can be obtained from the golden-rule expression using the third-order perturbative term for the t matrix:

$$t_{f\leftarrow i}=\sum_{m_1,m_2}\frac{\langle f\,|\,H\,|\,m_2\rangle\langle m_2\,|\,H\,|\,m_1\rangle\langle m_1\,|\,H\,|\,i\rangle}{(E_i-E_{m_1}+is)(E_i-E_{m_2}+is)}\,, \tag{1}$$

where i, f, m_1, and m_2 are the initial, final, and intermediate states with energies E_n ($n=i, f, m_1$, and m_2), H is a Hamiltonian that is a sum of the electronic intersite coupling Hamiltonian and the single-site phonon Hamiltonians, and s is a positive infinitesimal. For this work, f is state E_{1b} and i is state E_{1a}, but there are many different possibilities for the intermediate states that each gives rise to a separate term in the final expression. The one constraint on the intermediate states is that a phonon must be absorbed before a second phonon can be emitted. The states involved in the important processes are sketched in Fig. 2. They correspond to all the allowed time orderings of the intersite coupling and single-site phonon interactions. Following the earlier treatment,[2] Eq. (2) can be obtained for the rate

$$\omega_{\rm res}=\frac{C}{\delta^2}\left[(J_1^2+J_4^2+J_5^2)(\Delta_{E_{2a}}+\delta)^3\frac{n(\Delta_{E_{2a}}+\delta)+1}{n(\Delta_{E_{2a}})+1}n(\Delta_{E_{2a}})+(J_1^2+J_2^2+J_4^2)(\Delta_{E_{2b}}-\delta)^3 n(\Delta_{E_{2b}}-\delta)\right.$$
$$\left.+(J_1^2+J_2^2+J_3^2)(\Delta_{Z_{2b}}+\delta)^3\frac{n(\Delta_{Z_{2b}}+\delta)+1}{n(\Delta_{Z_{2b}})+1}n(\Delta_{Z_{2b}})+(J_1^2+J_3^2+J_5^2)(\Delta_{Z_{2a}}-\delta)^3 n(\Delta_{Z_{2a}}-\delta)\right], \tag{2}$$

where

$$C=\frac{3A^2}{2\pi\rho\hbar^4}\left[\sum_s\frac{\alpha_s}{v_s^5}\right],$$

A is the coupling constant for the strain operator (which is assumed to be constant independent of the states or sites involved), ρ is the density, α_s and v_s are a constant and the phonon velocity for the s polarization of an acoustical phonon, $n(\Delta_A)$ is the Bose factor for phonon occupation at an energy Δ_A of state A relative to the state below it, δ is the energy difference between the final and initial states, and the J_i are the electronic coupling constants for the energy-transfer transitions between the ion pairs states $(E_{1a},Z_{1b})\rightarrow(Z_{1a},E_{1b})$, $(E_{1a},Z_{2b})\rightarrow(Z_{1a},E_{2b})$, $(E_{1a},Z_{2b})\rightarrow(Z_{2a},E_{1b})$, $(E_{2a},Z_{1b})\rightarrow(Z_{1a},E_{2b})$, and $(E_{2a},Z_{1b})\rightarrow(Z_{2a},E_{1b})$ for $i=1\rightarrow5$, respectively (see Ref. 3). We have assumed that δ is much larger than the linewidths of the states and that the phonon density of states can be described by a Debye distribution.

Each term in Eq. (2) represents the contribution of the processes sketched in Fig. 2. The processes are grouped by numbers that correspond to the individual terms in Eq. (2). Each term has a phonon population factor corresponding to the absorption of a phonon. The phonon energy is $\Delta_{E_{a2}}$, $(\Delta_{E_{2b}}-\delta)$, $\Delta_{Z_{2b}}$, and $(\Delta_{Z_{2a}}-\delta)$ for terms 1 through 4, respectively (or processes 1 through 4 in Fig. 2). There is also a ratio of phonon population factors corresponding to the emission of phonons. One factor corresponds to the phonon emission represented in Fig. 2, while the other represents an alternative phonon emission that leads only to relaxation of the excited level and causes the phonon broadened linewidth of the upper level. The ratio of the two population factors reflects the branching ratio of the two processes after phonon excitation. Note that the branching ratio of terms 2 and 4 is unity because the phonon emission required for energy transfer and intraion phonon relaxation is the same. Each term is weighted by the cube of the phonon energies involved and reflects the phonon density of states at those energies.

The transient populations expected from excitation of either level E_{1a} or E_{1b} in Fig. 1 can be described by two coupled rate equations where the energy-transfer rate between the levels, $W_{E_{1a}E_{1b}}$ or $W_{E_{1b}E_{1a}}$, can be described by a unique rate constant:

$$\dot{N}_{E_{1a}}=-(W_{E_{1a}}+W_{E_{1a}E_{1b}})N_{E_{1a}}+W_{E_{1b}E_{1a}}N_{E_{1b}}\,, \tag{3}$$

$$\dot{N}_{E_{1b}}=-(W_{E_{1b}}+W_{E_{1b}E_{1a}})N_{E_{1b}}+W_{E_{1a}E_{1b}}N_{E_{1a}}\,. \tag{4}$$

Here, W_A and N_A are the rate constant for single-ion relaxation and the population of state A. The solution of these equations for the condition where level E_{1a} is initially excited to a population $N^0_{E_{1a}}$ is[17]

$$N_{E_{1a}}(t)=\frac{N^0_{E_{1a}}}{S}\left[\frac{(S-R)}{2}\exp[-(T-S)t/2]+\frac{(S+R)}{2}\exp[-(T+S)t/2]\right], \quad (5)$$

where

$$R=(W_{E_{1a}}+W_{E_{1a}E_{1b}})-(W_{E_{1b}}+W_{E_{1b}E_{1a}}),$$

$$S=(R^2+4W_{E_{1a}E_{1b}}W_{E_{1b}E_{1a}})^{1/2},$$

$$T=(W_{E_{1a}}+W_{E_{1a}E_{1b}})+(W_{E_{1b}}+W_{E_{1b}E_{1a}}).$$

At low temperatures where the back-transfer rate, $W_{E_{1b}E_{1a}}$, is small, expression (5) reduces to a single exponential with a decay rate $(W_{E_{1a}}+W_{E_{1a}E_{1b}})$. At higher temperatures where the transfer rates become much larger than $W_{E_{1a}}$ or $W_{E_{1b}}$, expression (5) has two exponential decays—a slow one with a rate of

$$(W_{E_{1b}}W_{E_{1a}E_{1b}}+W_{E_{1a}}W_{E_{1b}E_{1a}}/W_{E_{1a}E_{1b}}+W_{E_{1b}E_{1a}})$$

and a rapid one with a rate of $(W_{E_{1a}E_{1b}}+W_{E_{1b}E_{1a}})$. Similar expressions can be obtained for the population of level E_{1b} after direct excitation or excitation of E_{1a}.

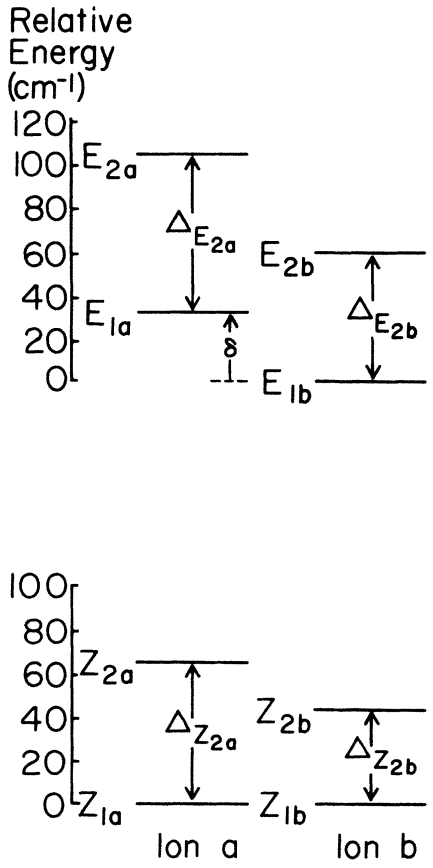

FIG. 1. Relevant energy-level structure for the a and b ions of the K site in SrF_2:Er^{3+}. The upper (E) and lower (Z) levels belong to the $^4S_{3/2}$ and $^4I_{15/2}$ manifolds, respectively.

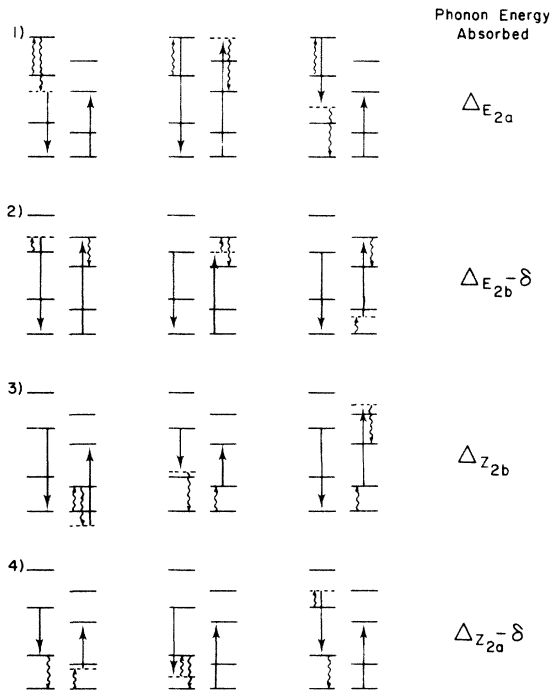

FIG. 2. The important Orbach processes described by Eq. (2) for the K site. See text for details.

In order to extract the energy-transfer rate from the transient, it is necessary to know the relative size of the single-ion relaxation rates $W_{E_{1a}}$ and $W_{E_{1a}E_{1b}}$, and the rates $W_{E_{1b}}$ and $W_{E_{1b}E_{1a}}$. $W_{E_{1b}}$ can be readily measured at low temperatures where it is the only rate which significantly contributes to the depopulation of E_{1b}, and is given by the lifetime of level E_{1b} after direct excitation. The rate $W_{E_{1b}E_{1a}}$ is not directly measured, but is very small at low temperatures. It is related to the reverse rate, $W_{E_{1a}E_{1b}}$, by detailed balance:

$$W_{E_{1b}E_{1a}}=W_{E_{1a}E_{1b}}e^{-\delta/kT}. \quad (6)$$

The relative size of $W_{E_{1a}}$ and $W_{E_{1a}E_{1b}}$ can be obtained from the ratio of the fluorescence intensity from level E_{1b} when it is excited indirectly through level E_{1a} $[I_{E_{1b}}(E_{1a})]$ to that when it is excited directly $[I_{E_{1b}}(E_{1b})]$ since

$$\frac{I_{E_{1b}}(E_{1a})}{I_{E_{1b}}(E_{1b})}=K\frac{W_{E_{1a}E_{1b}}}{W_{E_{1a}}+W_{E_{1a}E_{1b}}}\frac{N^0_{E_{1a}}}{N^0_{E_{1b}}}, \quad (7)$$

where N^0 represents the initial populations established in levels E_{1a} or E_{1b} and K is a constant containing many factors that relate level populations to the experimentally measured fluorescence intensity. Equation (7) is obtained by integrating the fluorescence transients for the two excitation energies over the entire transient and is rigorous

even if back transfer is important. Since the transfer rate $W_{E_{1a}E_{1b}}$ is strongly temperature dependent and rapidly becomes much larger than $W_{E_{1a}}$, the ratio $I_{E_{1a}}(E_{1b})/I_{E_{1b}}(E_{1b})$ approaches $KN^0_{E_{1a}}/N^0_{E_{1b}}$ as the temperature is raised. At low temperatures, $(T+S)/2$ in Eq. (5) becomes $(W_{E_{1a}}+W_{E_{1a}E_{1b}})$ and can be directly measured from the transient obtained by exciting level E_{1a} and measuring its fluorescence. The value of $W_{E_{1a}}$ can be obtained by fitting the measured ratio $I_{E_{1b}}(E_{1a})/I_{E_{1b}}(E_{1b})$ with Eq. (7) as a function of $(W_{E_{1a}}+W_{E_{1a}E_{1b}})$. The energy-transfer rate can then be found at any temperature by measuring the fluorescence decay rate from level E_{1a} after direct excitation and extracting $W_{E_{1a}E_{1b}}$.

EXPERIMENTAL

The fluorescence transients observed in this work were excited with a nitrogen laser-pumped dye laser which had approximately 0.01-nm bandwidth. Fluorescence was measured with an RCA C31034A photomultiplier and either a Biomation 802 transient recorder for transients with greater than 10 μs lifetimes or a Biomation 805 transient recorder for shorter transients. Individual transients were signal averaged with a small laboratory computer. The fluorescence was excited in a SrF_2:0.1 mol% Er^{3+} crystal obtained from Optovac, Inc. Three methods were used to cool the crystal. For the (2—4.2)-K range, the crystal was immersed in pumped liquid helium. The crystal temperature was measured by determining the vapor pressure above the liquid helium. Temperatures in the (7—27)-K range were obtained by mounting the crystal in a flowing stream of helium gas provided by a commercial transfer refrigerator. The temperature was measured with a Chromel-gold (0.07 at.% Fe) thermocouple that was mounted directly after the crystal. The thermocouple was calibrated by direct immersion in liquid helium and liquid nitrogen. Temperatures above 11 K were obtained with a closed-cycle refrigerator. The crystal temperature was measured spectroscopically from the fluorescence intensity ratio of the J-site $^4S_{3/2}$ manifold transitions. The J site $^4S_{3/2}$ manifold is split by 21 cm^{-1} and the relative intensity of transitions from each level is determined by the Boltzmann equation (16). The intensity ratio was measured when the crystal was immersed in liquid-nitrogen temperature in order to calibrate the relative intensity measurement. Measurements made by cooling the crystal in a helium gas flow agreed with measurements made with the closed-cycle refrigerator in the overlapping temperature range.

RESULTS

The fluorescence transients of the E_{1a} level after direct excitation are shown in Fig. 3 for a series of temperatures. At low temperatures, the decay is exponential with a rate constant of $\omega_{E_{1a}}+\omega_{E_{1a}E_{1b}}$ since back transfer is unimportant. As the temperature is raised, the rate increases because of the $\omega_{E_{1a}E_{1b}}$ temperature dependence and a second exponential decay becomes apparent with a slower rate. At high temperatures where back transfer is large, the two contributions become equal at early times. Figure 3(d) shows explicitly the two contributions to the transient. Equation (5) describes the transients within the limits of measurement. The presence of back transfer complicates the analysis because the overall rate constant obtained by fitting the transients is given by the complex combination of the individual rate constants in Eq. (5).

An $\omega_{E_{1b}}$ value of 1030 s^{-1} is obtained by measuring the lifetime of the E_{1b} level at low temperatures where back transfer is unimportant. The value of $\omega_{E_{1a}}$ was obtained from the temperature dependence of the $I_{E_{1b}}(E_{1a})/I_{E_{1b}}(E_{1b})$ ratio. The measured ratio is shown in Fig. 4 as a function of the rate measured for the E_{1a} level transient. At low temperatures, this rate is $(\omega_{E_{1a}}+\omega_{E_{1a}E_{1b}})$. The ratio was fit to Eq. (7) with $\omega_{E_{1a}}$ as an adjustable parameter. For any given temperature, the ratio of the forward- and back-transfer rates ($\omega_{E_{1a}E_{1b}}$ and $\omega_{E_{1b}E_{1a}}$) was known from Eq. (6). The rate $\omega_{E_{1a}E_{1b}}$ for any temperature was obtained by finding the value needed to make $(T-S)/2$ in Eq. (5) match the measured rate for the transient. This procedure corrects for back transfer although the back transfer contributes little to the determination. It is only important at high temperatures where the curve is flat

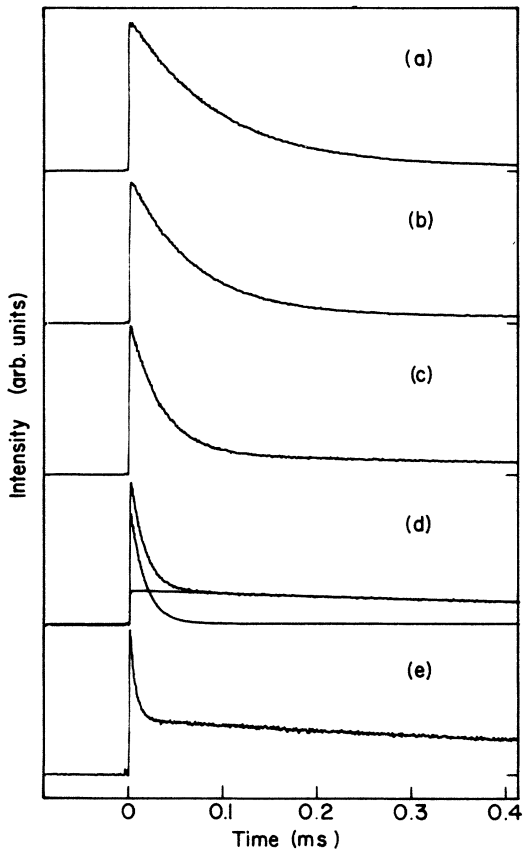

FIG. 3. Fluorescence transients of the E_{1a} level after direct excitation at (a) 11, (b) 16, (c) 23, (d) 32, and (3) 43 K.

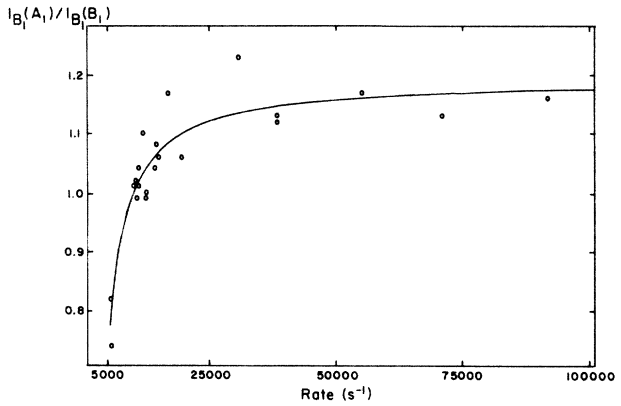

FIG. 4. Measured excitation ratio $I_{E_{1b}}(E_{1b})/I_{E_{1b}}(E_{1a})$ as a function of rate measured for the E_{1a} level. The curve is the best fit of Eq. (7) to the data.

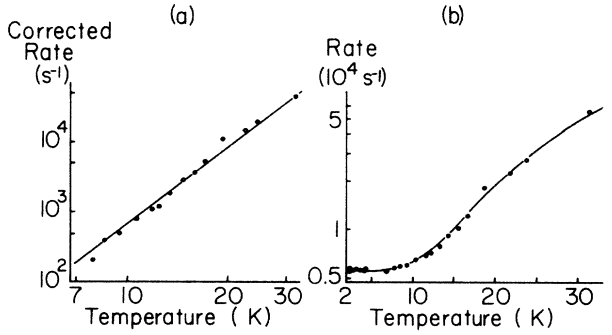

FIG. 5. (a) Temperature dependence of the transfer rate after correction for the direct process. The line shows the best fit for a two-phonon nonresonant process with dependence, T^n, $n=3.6$. (b) Temperature dependence of the observed rates $(\omega_{E_{1a}}+\omega_{E_{1a}E_{1b}})$. Line is the best fit of Eq. (2) plus contributions from the direct process and single-ion relaxation.

and insensitive to the value chosen. Once $\omega_{E_{1a}E_{1b}}$ was known, Eq. (7) could be used to predict the intensity ratio. This procedure was followed to obtain the solid curve shown in Fig. 4. The best fit occurred for an $\omega_{E_{1a}}$ value of 1920 s^{-1}

The observed rates can now be corrected for back transfer using Eq. (5) to give the rate $\omega_{E_{1a}E_{1b}}$ as a function of temperature. The results for the corrected rate, $\omega_{E_{1a}E_{1b}}$, plus the single-ion relaxation rate, $\omega_{E_{1a}}$, which we assume is independent of temperature, are shown in Fig. 5(b). This rate is relatively constant at low temperatures but increases sharply above 10 K. The limiting rate at very low temperatures is 5430 s^{-1}, much larger than the 1920-s^{-1} rate for $\omega_{E_{1a}}$. There must therefore be a temperature-independent component of 3510-s^{-1} rate for $\omega_{E_{1a}E_{1b}}$.

The different mechanisms for nonresonant energy transfer predict different temperature dependences. The one-phonon-assisted process has only a slight temperature dependence in this region, but since it is the only mechanism that predicts a finite transfer rate at low temperatures, the 3510-s^{-1} rate must be due to the one-phonon-assisted process. The temperature dependence of this process is well known and follows a $1/(1-e^{-\delta/kT})$ dependence for the conditions of these experiments. The rates at higher temperature were calculated from the low-temperature rate and subtracted from the data to leave the contribution to the energy transfer from higher-order phonon processes. The temperature dependence of the corrected rate is shown in Fig. 5(a).

Two-phonon-assisted nonresonant processes involving two-site and one-site Raman interactions have a temperature dependence between T^3 and T^7 depending upon the phonon phase interference effects and assuming that the temperature is low compared to the Debye temperature. Previous experiments found rates that varies as $T^{4.3.6}$. Figure 5(a) shows the fit of $\log_{10}\omega_{E_{1a}E_{1b}}$ to AT^n where A and n are adjustable parameters. The best fit to the data gave a value for $n=3.6$. The fit is excellent at all points but the lowest temperatures where the measured rates are lower than the predicted rates.

The temperature dependence of the two-phonon-assisted resonant Orbach process is given by Eq. (2). All of the energies in this equation are known spectroscopically. We assume further that the electron coupling constants are all identical so the entire fit of Eq. (2) to the data can be controlled by adjusting the size of C. Figure 5(b) shows the results of the fit to the measured rates. Again, the rate of the one-phonon direct process that was determined at low temperatures has been added to Eq. (2) in order to account for that contribution to the measured rates. The dominant contribution to the energy transfer over this temperature range comes from the third term in Eq. (2), both because the phonon population is significant and the term is weighted favorably by the phonon density at the particular phonon energy. The fit could be improved slightly if the first term was weighted somewhat less and the second or fourth terms were weighted more favorably. The 104.2-cm^{-1} phonon energy required for the processes represented by the first term lies somewhat above the region where a Debye distribution is appropriate,[18] so one might expect it to have less weight than that predicted by a Debye distribution. Similarly, differences in the magnitudes of the electronic or strain coupling constants can change the relative weights. Nevertheless, the changes caused by these considerations are not significant enough in comparison with the data to warrant their inclusion in the fitting.

The fits for the nonresonant and resonant two-phonon processes are excellent and cannot be used to distinguish between either mechanism. The Orbach process fits the data around 10 K significantly better while the nonresonant two-phonon processes continue to fit the dependence at higher temperatures than those shown, where additional resonant Orbach processes become possible from thermally populated states. In order to distinguish between the two mechanisms, we examined the dependence of the transfer rate on magnetic field. The Orbach process should depend strongly on the energy difference with the resonant level [see Eq. (2)], but the nonresonant two-phonon processes should have little dependence.

A magnetic field of 25 kG was applied along the [110] axis and the lifetimes were measured at 8 and 20 K. At 8 K, the lifetime changed from 173 μs without the field to 137 μs with the field. At 20 K, the lifetime changed from 42.3 μs to 18.4 μs. The contribution by the Orbach process can be obtained by subtracting the temperature-independent rate (1920 s^{-1}) and the weakly temperature-dependent single-phonon-assisted rate from the total rates corrected for back transfer. One then finds the rates have increased from 340 to 1860 s^{-1} at 8 K and 15 700 to 43 600 s^{-1} at 20 K as a result of the field. There cannot be an appreciable field-independent component to these rates from nonresonant two-phonon processes because the increase in the rate is so large. The increase in the rate is difficult to predict because there are a number of terms that contribute to Eq. (2) and there are many more levels involved because of the Zeeman splittings. The third term contributes the largest amount and the value of $\Delta_{Z_{2b}}$ also has the greatest change with field from 44 cm^{-1} without the field to 35 cm^{-1} with the field. One cannot get accurate values for the other splittings because the available fields do not resolve the entire Zeeman patterns. Nevertheless, estimates using only the third term predict the rate should increase by a factor of 5 at 8 K and 2 at 20 K. The observed increases of 5.5 and 2.8 are appreciably larger and indicate there can be little contribution from a nonresonant process. The estimated rates are also underestimated because the phonon resonances are approximated by δ functions in the usual derivation, and the level separations in this system are not large compared with the linewidths.[4]

The ratio of the rate from Orbach transfer to that from direct one-phonon-assisted transfer can be written[7]

$$\frac{\omega_{\rm res}}{\omega_{\rm dir}} = \frac{3|A|^2}{2(f-g)^2}\frac{(\Delta_{Z_{2b}}+\delta)^3}{\delta^3} \times \frac{n(\Delta_{Z_{2b}}+\delta)+1}{[n(\Delta_{Z_{2b}})+1][n(\delta)+1]} n(\Delta_{Z_{2b}}) , \quad (8)$$

where $|A|^2$ is the coupling constant for the strain operator between the electronic states involved in the resonant phonon interactions and $(f-g)^2$ is the difference in coupling constants of the strain operator for the electronic states involved in the direct phonon process assuming that the processes associated with the third term in Eq. (2) are dominant. By comparing Eq. (8) with the data, we find that $|A|^2/(f-g)^2=6$. One would expect $|A|^2$, f^2, and g^2 to have comparable values, but the $|A|^2/(f-g)^2$ ratio would have a value larger than 1 because of the cancellation that occurs in the denominator. Thus, the Orbach and direct one-phonon processes have an appropriate relative magnitude in this system. Similar comparisons in ruby did not give results that could be readily understood.[7]

There is no indication that a nonresonant two-phonon process is important in the SrF_2:Er^{3+} system. Such a process has only a weak dependence on the energy mismatch when kT is large compared to the mismatch.[1-3] The dependence at the mismatch values for the SrF_2:Er^{3+} system is weak[3] and thus one would anticipate that the Orbach process would dominate the energy transfer at small energy mismatches as well. The failure to observe the Orbach process in the PrF_3 and LaF_3:Pr^{3+} systems[4,6] arose because these systems do not have appropriate levels for phonon resonances. The $^3P_0$ state that was studied by fluorescence line narrowing is a singlet state. The ground $^3H_4$ manifold has a crystal-field level at 57 cm^{-1},[19] but this energy difference is too large to contribute in the temperature range of the experiments that were performed.[4,6] An Orbach energy-transfer process should play an important role in systems where there are excited levels that can participate in resonant phonon processes.

ACKNOWLEDGMENTS

We would like to acknowledge the helpful conversations we have had with Professor David Huber and Frank Imbusch. We would like to thank Professor Fleming Crim for the loan of his Biomation Model No. 805 transient recorder. This research was sponsored by the U.S. National Science Foundation under Grants No. DMR-8205145 and No. DMR-8513705.

*Present address: Los Alamos National Laboratories, Los Alamos, NM 87545.

[1]T. Holstein, S. K. Lyo, and R. Orbach, Phys. Rev. Lett. **36**, 891 (1976).

[2]T. Holstein, S. K. Lyo, and R. Orbach, Phys. Rev. B **15**, 4693 (1977).

[3]T. Holstein, S. K. Lyo, and R. Orbach, *Laser Spectroscopy of Solids,* edited by W. M. Yen and P. M. Selzer (Springer-Verlag, Berlin, 1981), Vol. 49.

[4]R. Flach, D. S. Hamilton, P. M. Selzer, and W. M. Yen, Phys. Rev. Lett. **35**, 1034 (1975).

[5]P. M. Selzer, D. S. Hamilton, and W. M. Yen, Phys. Rev. Lett. **38**, 858 (1977).

[6]D. S. Hamilton, P. M. Selzer, and W. M. Yen, Phys. Rev. B **16**, 1858 (1977).

[7]P. M. Selzer, D. L. Huber, B. B. Barnett, and W. M. Yen, Phys. Rev. B **17**, 4979 (1978).

[8]A. Monteil and E. Duval, J. Phys. C **13**, 4565 (1980).

[9]A. Monteil and E. Duval, J. Phys. C **17**, 5219 (1984).

[10]I. Y. Chan and B. L. Goldenberg, J. Chem. Phys. **79**, 3711 (1983).

[11]L. D. Merkle and R. C. Powell, Phys. Rev. B **20**, 75 (1979).

[12]M. Zokai, R. C. Powell, G. F. Imbusch, and B. DiBartolo, J. Appl. Phys. **50**, 5930 (1979).

[13]W. B. Smith and R. C. Powell, J. Chem. Phys. **76**, 854 (1982).

[14]R. S. Meltzer, J. E. Rives, and W. C. Egbert, Phys. Rev. B **25**, 3026 (1982).

[15]S. A. Basun, A. A. Kaplyanskii, and S. P. Feofilov, Fiz.

Tverd. Tela (Leningrad) **26**, 1808 (1984) [Sov. Phys.—Solid State **26**, 1093 (1984)].
[16]M. D. Kurz and J. C. Wright, J. Lumin. **15**, 169 (1977).
[17]B. DiBartolo, *Optical Interactions in Solids* (Wiley, New York, 1968), p. 442.
[18]M. M. Elcombe, J. Phys. C **5**, 2702 (1972).
[19]E. Y. Wong, O. M. Stafsudd, and D. R. Johnson, J. Chem. Phys. **39**, 786 (1963).